SCIENTIFIC REPORTS

OPEN

$Ni(OH)_2$-decorated nitrogen doped MWCNT nanosheets as an efficient electrode for high performance supercapacitors

Received: 5 November 2018
Accepted: 22 February 2019
Published online: 15 April 2019

Sivalingam Ramesh[1], K. Karuppasamy[2], Hemraj M. Yadav[3], Jae-Joon Lee[3], Hyun-Seok Kim[2], Heung-Soo Kim[1] & Joo-Hyung Kim[4]

In this study, nickel hydroxide nanoparticles (NPs) decorated with nitrogen doped multiwalled carbon nanotubes (N-MWCNT) hybrid composite was synthesized by thermal reduction process in the presence of cetyl ammonium bromide (CTAB) and urea. The as-synthesized $Ni(OH)_2$@N-MWCNT hybrid composite was characterized by FTIR, Raman, XRD, BET, BJH and FE-TEM analyses. These prepared porous carbon hybrid composite materials possessed high specific surface area and sheet like morphology useful for active electrode materials. The maximum specific capacitance of $Ni(OH)_2$@N-MWCNT hybrid nanocomposite in the two electrode system showed 350 Fg^{-1} at 0.5 A/g, energy density ~43.75 Wkg^{-1} and corresponds to power density 1500 W kg^{-1} with excellent capacity retention after 5000 cycles. The results suggest that the prepared two-dimensional hybrid composite is a promising electrode material for electrochemical energy storage applications.

Supercapacitors or ultra-capacitors are energy storage devices that have higher power density and better cyclic stability than conventional batteries. They are used as the most promising electrochemical energy storage devices with potential to eventually replace batteries for high-performance energy storage applications. Hybrid composites have been widely utilized in portable electronics, hybrid vehicles and backup energy systems for high-performance applications[1–3]. Based on energy storage mechanisms and properties, the supercapacitors can be classified into electric double layer (EDLCs) and pseudocapacitors[4–6]. In EDLCs, the electrodes generally consist of various forms of carbon, including activated carbons, carbon nanotubes, graphene and porous materials for supercapacitors[7–9]. Redox capacitors or pseudocapacitors employ transition metal oxides or conducting polymer as electrode materials.

In EDLCs, the energy storage mechanism involves electrostatic accumulation of charges at electrode-electrolyte interface between the electrode and ionic charges in the electrical double layer. However, in pseudo capacitors, stored energy is released in presence of reversible redox reactions or faradaic reactions occurring in electroactive materials. In addition, in EDLCs, capacitance is originated from a collection of charges at the electrode-electrolyte interface. To increase electrical conductivity and achieve high storage capacity, specific surface area and pore sizes are very important in EDLCs. Various graphene and carbon nanotubes structured composites have been widely used for electrochemical energy storage applications[7–9].

The currently, recent developments of asymmetric supercapacitor is mainly focused on synthesis, properties, and performances of the state of the art materials for anode and cathodes in the supercapacitor applications. Mainly, the carbon-based materials such as porous carbon, activated carbon, carbon nanotubes, graphene, and graphene oxide materials are generally used for negative electrodes due to their high surface area and electrostatic charge-storage mechanisms at electrode/electrolyte interfaces. In particular, the pseudo capacitance of some metal oxides and nitrides have also been utilized as anode materials. The positive electrode containing the

[1]Department of Mechanical, Robotics and Energy Engineering, Dongguk University –Seoul, Pil-dong, Jung-gu, 04620, Seoul, South Korea. [2]Division of Electronics and Electrical Engineering, Dongguk University –Seoul, Pil-dong, Jung-gu, 04620, Seoul, South Korea. [3]Department of Energy and Materials Engineering, Dongguk University –Seoul, Pil-dong, Jung-gu, 04620, Seoul, South Korea. [4]Department of Mechanical Engineering, Inha University, 100, Inha-ro, Nam-gu, Incheon, 22212, South Korea. Correspondence and requests for materials should be addressed to H.-S.K. (email: heungsoo@dgu.edu) or J.-H.K. (email: joohyung.kim@inha.ac.kr)

pseudocapacitive behaviours metal oxides and include carbonaceous materials. In addition, the electrode materials are design in the various nanostructured morphology of nanospheres, nanosheets, nanorods, nanowires, and nanoribbons. Recently, the studied two-dimensional materials such as transition metal dichalcogenides and transition-metal carbides for used in the current filed of supercapacitor applications[10].

The asymmetric supercapacitors are an effective approach for extending the operating voltage window of the powder sources for supercapacitor and battery applications. These supercapacitor generally consists of a battery-type Faradic electrode (used as cathode) as an energy source and a capacitor-type electrode (anode) is a power source. Therefore, the asymmetric technology is expected to achieve an increased energy density and high cell voltage and improving the capacitance of cathode and anode materials have been widely studied. The carbon based materials are frequently used as anode in asymmetric supercapacitors. Because of the lower specific capacitance of carbon materials severely limits the energy density for supercapacitor for two electrodes. Metal oxide based anodes with nanostructures, such as MnO_2, NiO, Co_3O_4, and Fe_2O_3, are promising electrode materials for asymmetric supercapacitors because of their high specific capacitance, two or three times higher than that of carbon/graphite-based materials[11].

Based on these asymmetric electrode properties, the carbon nanotubes (CNTs) and reduced graphene oxide materials have also attracted significant attention in the field of biosensor, supercapacitor and electro catalytic applications due to their inherent potential properties of chemical stability, conductivity, flexibility, excellent catalytic activity and fast electron transfer reactions[12–15]. To improve the conducting property and surface area of MWCNT, nitrogen (N) was doped into the carbon matrix of MWCNT in the present investigation. Such N-doped process is very important for new generation of metal-free catalysts for electrochemical reactions. Nitrogen valence electrons are incorporated to the graphitic plane while π-electrons are generated in the carbon surface[16]. This may be due to π-electrons generation together with significant difference in electronegativity between nitrogen and carbon atoms. Therefore, the carbon-based materials contains unique properties such as high surface energy and polarization effect. N-doping can also improve both reactivity and electro catalytic performance of carbon materials. Therefore, *in-situ* doping involves direct incorporation of N atoms into carbon materials during the synthesis process in the presence of suitable catalyst.

Nickel oxide (NiO) is an important transition metal oxide that has attracted great interest due to its extensive applications in fields of catalysis, sensors and renewable energy sources[14–16]. A plenty of studies have been investigated the active electrode materials used like CuO, NiO, MnO_2, $Co(OH)_2$ and $Ni(OH)_2$ for supercapacitors[16–22]. Amongst, nickel hydroxide, $Ni(OH)_2$ materials have paid great attention due to their widely potential applications in alkaline rechargeable batteries, portable electronics and electric vehicles[2]. Further, it contains α and β phases. The crystalline β-$Ni(OH)_2$ electrodes have been widely used for electrochemical applications due to their higher stacking density and stability when compared to α-$Ni(OH)_2$. Numerous electrochemical studies have been reported the $Ni(OH)_2$ electrodes on various carbon materials shows an improved electrochemical performance with excellent cyclic stability[23–26]. Electrochemical properties of $Ni(OH)_2$/CNTs hybrid composite could be improved the specific capacitance and cyclic stability in presence of strong electrolyte like KOH at different concentrations. The electrochemical properties of $Ni(OH)_2$/CNTs composite shows various specific capacitances and excellent stability of electroactive carbon materials have been shown[27]. Additionally, Ni $(OH)_2$/MWCNTs hybrid nanocomposite can provide one-dimensional (1D) nanostructure owing to its high specific capacitance and excellent cycling stability and unusual electrical conducting properties.

Based on previous studies[28,29], hybrid nanocomposites with different morphology based electrode materials have been synthesized for high-performance supercapacitors with excellent cyclic stability. In the present study, nanostructured nickel hydroxide oxide decorated N-MWCNT hybrid composite electrodes were synthesized and characterized for utilization in high performance supercapacitors for the first time. Systematic morphology and structural analyses revealed that the prepared hybrid electrode possessed high surface area with uniform pore size. Electrochemical properties of $Ni(OH)_2$ @N-MWCNT hybrid composite (two and three) electrodes are displayed a high specific capacitance of two electrode is ~350 Fg^{-1} at 0.5 A/g and the detailed analyses are discussed below.

Results and Discussion

Structural results of the hybrid composite. The Schematic illustration of step by step synthesis of $Ni(OH)_2$@N-MWCNT hybrid electrode is demonstrated in Fig. 1. The various structural interactions and complexation properties between N-MWCNT and $Ni(OH)_2$ of the hybrid composite were analyzed through FTIR spectroscopy. The hybrid composite results are displayed in Fig. 2a. A broad band was observed at ~3495 cm^{-1}. It could be represented to the stretching frequency of $Ni(OH)_2$ present in the hydrogen bonded hydroxyl groups. The peaks appeared at 2844–2909 cm^{-1}, indicating CH_2 stretching mode from CTAB surfactant and other important functional modes such as C=O, C-H bending, C-O stretching, C-O-C stretching observed at 1631, 1476, 1357 and 1162 cm^{-1} respectively. There was a strong vibrational band in the region between 650 and 550 cm^{-1}, especially at 598 cm^{-1} corresponding to Ni-O bond of $Ni(OH)_2$. These results strongly suggest the presence of $(NiOH)_2$ in the hybrid composite structure. The hybrid composite results also further confirmed that $(NiOH)_2$ bonded to N-doped MWCNT surface in presence of CTAB surfactant and results compared to previous reports[28,30].

Raman spectra of hybrid composite are shown in Fig. 2b. There were two prominent peaks at 1287 cm^{-1} and 1604 cm^{-1} represent that the D and G peaks from N-doped MWCNT, respectively. Generally, the G band indicates in-plane bond stretching motion of carbon (C, sp2) atoms of (E2g phonons). In addition, the peaks position of 2575 cm^{-1} (D') and 2873 (2D) were also present in the hybrid nanostructure. The strong D band represents a large number of defects of N-doped MWCNT which is due to the reduction process of MWCNT. The intensity ratio of D and G peaks can be used to calculate disorder behaviours of carbon materials in sp2 domains[31]. The peak intensity of D and G are roughly calculated as (ID/IG = 1.08) represent that the large number of defects in

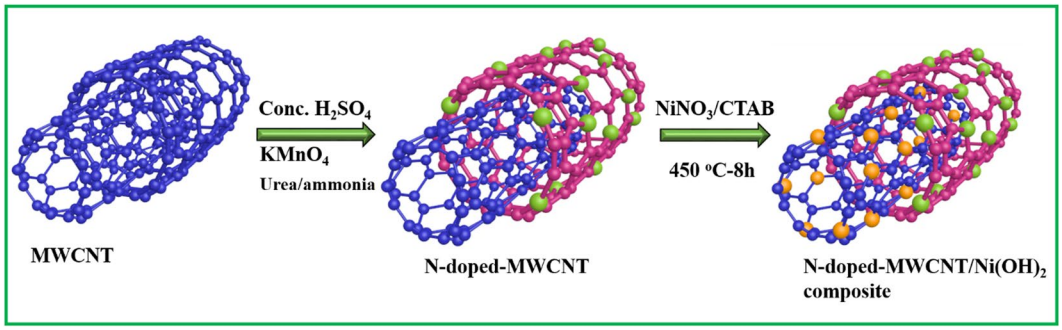

Figure 1. Schematic representation synthesis steps of Ni $(OH)_2$ @N-MWCNT hybrid composite.

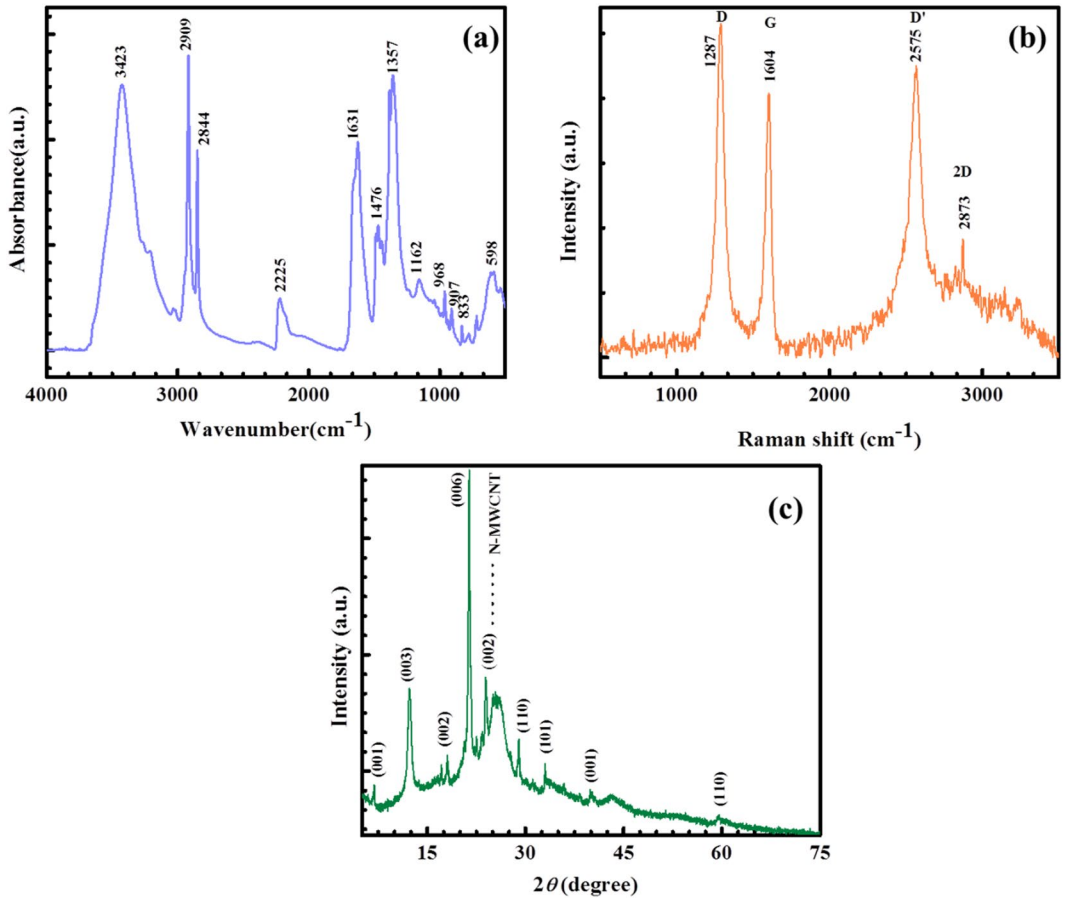

Figure 2. (**a**) FT-IR, (**b**) Raman and (**c**) XRD results of the hybrid composite.

the N-MWCNT surface. The peaks position at 3491 cm^{-1} and 2903 cm^{-1} are characteristic peaks of β-$Ni(OH)_2$. These Raman spectral results confirmed that $Ni(OH)_2$ was successfully anchored onto the surface of N-MWCNT.

Figure 2c represents XRD pattern of $Ni(OH)_2$@N-MWCNT hybrid composite. Diffraction peaks at 6.94°, 12.34°, 17.10°, 18.08°, 21.04°, 24.03°, 25.82°, 29.12°, 31.11°, 33.10°, 35.92°, 40.0°, 51.42° and 59.63° corresponded to (001), (003), (002), (006), and (110) planes of $Ni(OH)_2$@N-MWCNT surface confirmed by using standard JSPDS data (Card No. 14-0117).

All diffraction peaks showed hexagonal structure of $Ni(OH)_2$. There was no impurity in the hybrid composite. Therefore, the XRD peaks proved that thermal reduction process played an important role in improving the crystalline nature, consistent with previous reports[31–33].

Surface chemical compositions of $Ni(OH)_2$@N-MWCNT hybrid composite was analyzed by XPS. The XPS spectral results ranging from 0 to 1200 eV are shown in Fig. 3. Peaks at 855.65 and 872.90 eV indicates to Ni $2p^{3/2}$ and Ni $2p^{1/2}$ energy levels, respectively. Its corresponding fitting plot is represented in Fig. 4(a). Energy spin-energy separation of ~17.20 eV represented the characteristic of $Ni(OH)_2$ phase and further confirmed with a previous report[32]. In addition, O1s peaks at 532.12 eV are associated with bound hydroxide groups (OH),

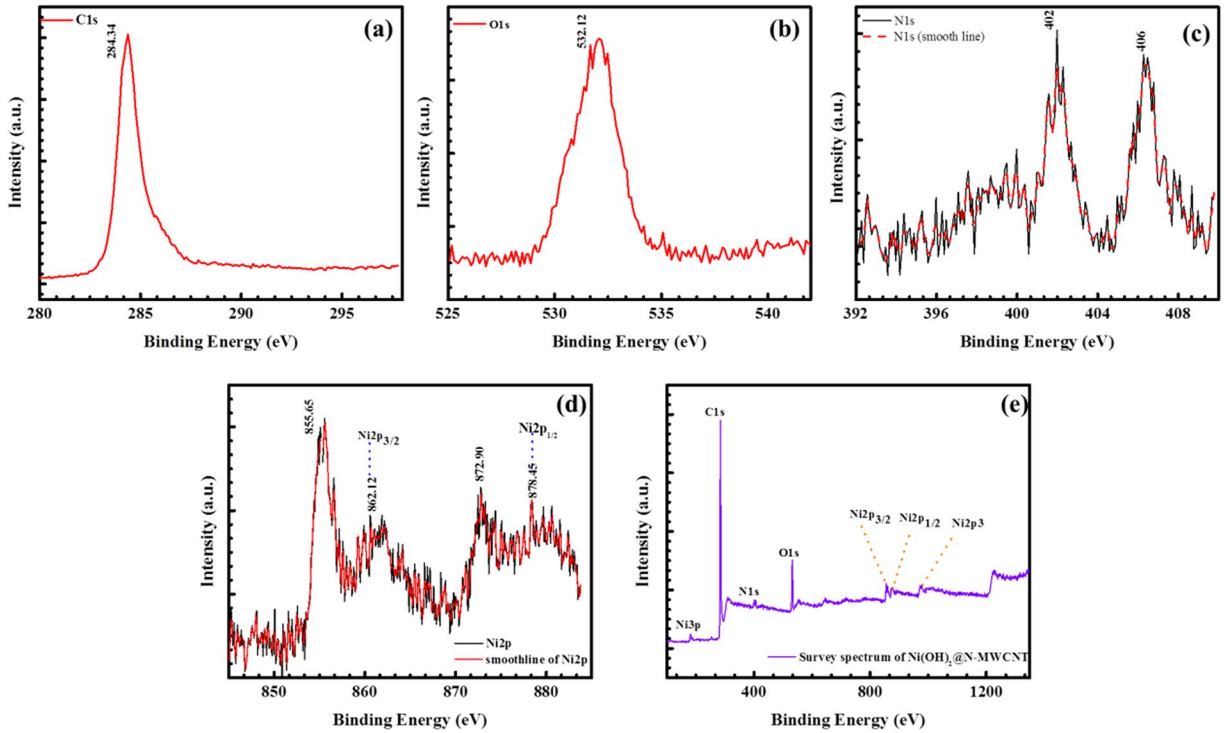

Figure 3. XPS results of (**a**) C1s, (**b**) O1s, (**c**) N1s, (**d**) $Nip^{3/2}$ and $Nip^{1/2}$ and (**e**) survey spectrum of the hybrid composite.

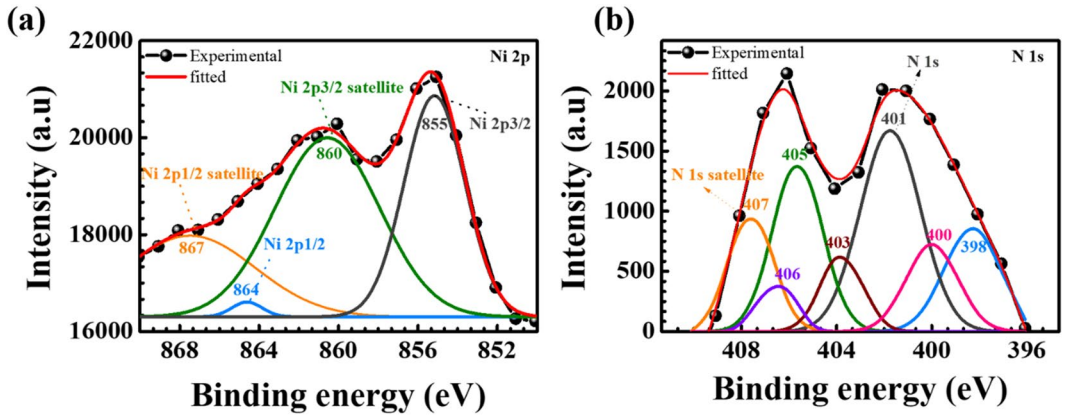

Figure 4. XPS fitting results of (**a**) Ni 2p and (**b**) N1s.

carbon (284.34 eV) and nitrogen (402–406 eV) (Fig. 4(b)) present in the hybrid composite structure confirmed the bonding between Ni $(OH)_2$ and n-doped MWCNT surface.

Surface and morphological properties. Figure 5 shows nitrogen adsorption/desorption isotherms of $Ni(OH)_2$@N-MWCNT hybrid composite samples at 77 K and analyzed by mesoporous materials. BET surface area of the hybrid composite was ~250 $m^2 g^{-1}$, then that of pristine nickel hybrid oxides (~108 $m^2 g^{-1}$)[34,35]. Pore size distribution of the hybrid composite showed very thin microspores and mesoporous of 0.5 to ~2.5 nm and macrospores below the ~200 nm. The hybrid composite showed a wide pore size distribution with particle size of ~1.5–20 nm. These mesopores and macropores of hybrid composite can facilitate the migration of K^+ and OH^- ions and enhanced the specific capacitance and cyclic stability in the electrochemical reactions[36].

Morphology and structure of Ni $(OH)_2$ @ N-MWCNT hybrid composite results were then studied by FE-TEM analysis. In these results (Fig. 6) of hybrid composite showed nanosheets like structure. The $Ni(OH)_2$ nanoparticles are densely decorated over the surface of N-MWNT. In certain areas, aggregated nanoparticles are occurred, this may be due to mixing of N-MWCNT and $Ni(OH)_2$. The SAED patterns corresponds to (003), (006), (110) and (002) patterns of $Ni(OH)_2$ are observed in the hybrid composite and also consistent with previous reports[37].

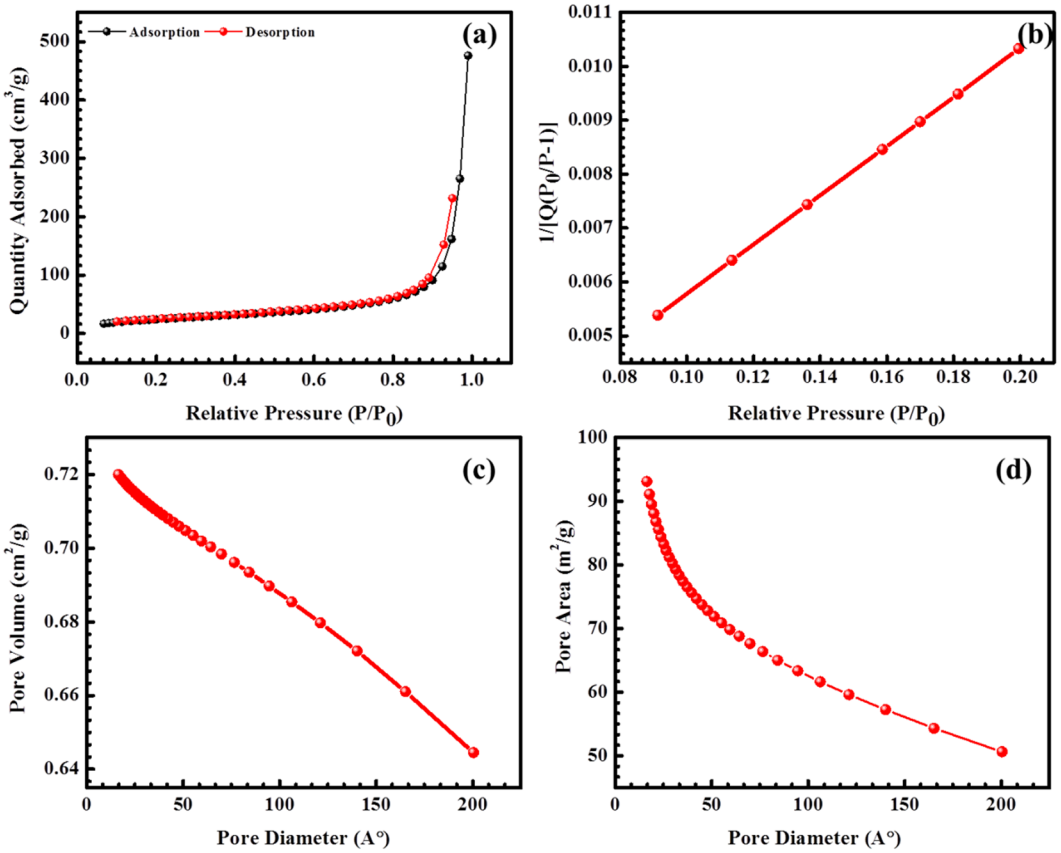

Figure 5. BET results of (**a**) adsorption-desorption, (**b**,**c**) pore volume and (**d**) pore area of the hybrid composite.

Electrochemical properties of the hybrid composite. Electrochemical properties of pristine nickel oxide, nickel hydroxides, carbon materials and metal oxides for supercapacitor applications have been widely reported in previous studies[37–39]. The metal oxides and metal hydroxides previous reports very clearly showed that the specific capacitance and cyclic stability increases due to various surface morphologies present in the hybrid composite[38,40]. In the present study, electrochemical properties of $Ni(OH)_2$@N-MWCMT hybrid composite was studied in the presence of 6 M KOH as electrolyte. Figure 7 shows CV profiles of Ni $(OH)_2$ @N-MWCNT hybrid composite at different scan rates (20 to100 mV/s) in the range of potential −0.2 to 0.8 V. The shape of CV loops for the hybrid composite electrode was close to a rectangular shape, indicating double layer capacity behaviour. The electrode showed a higher current density response than MWCNT, indicating its good charge storage performance. These results indicate that the overall capacitance of the electrode is increased because of $Ni(OH)_2$@N-MWCNT hybrid composite. Figure 7c shows results of galvanostatic charge–discharge tests of the electrode at different current densities form 3 to 6 A g^{-1}. Therefore, the hybrid composite showed a linear triangular-shaped curve, indicating a double-layer capacitive behaviour. Figure 7c shows specific capacitance versus current density plot. The hybrid composite showed specific capacitances of ~615, 560, 500 and 380 F·g^{-1} at different current densities from 3 to 6 A g^{-1}, respectively. The specific capacitance decreased when the applied current increased due to limited movement of electrolyte ions through electrodes. The composite exhibited higher capacitance (~615 F·g^{-1}) than pristine MWNT due to decoration of nickel hydroxides onto the surface of N-MWNT which effectively prevented agglomeration of MWNT. This may be due to increasing the ion transport and improving the EDLC behaviour of the electrode materials. Moreover, the composite showed capacitance of 380 F·g^{-1} when increases to 6 A·g^{-1}, indicating its excellent rate capability. The electrode showed only 10% capacitance loss after 5000 cycles at 3 A·g^{-1}, indicating its outstanding long-time stability. This might be due to its strong interaction with nickel hydroxides and N-MWCNT's rapid electron transfer and charge separation as well as its excellent conductive nature.

Typical Nyquist plots of $Ni(OH)_2$ @N-MWCNT hybrid composite electrode are shown in Fig. 7f. The plot consisted of a semicircle at high frequency region (0.1 Hz to 100 Hz). The internal resistance of the hybrid composite electrode in an open circuit condition was evaluated. In the high-to-medium frequency region, one semicircle was related to faradic reactions and charge transfer in the electrochemical reaction[41–45]. The charge transfer resistance was found to be 3.2 Ω and 15 Ω respectively, before and after cycling process which demonstrating the stable electrochemical performance nature of the prepared electrode material. Consequently, the low ESR value (straight line) in the low-frequency region might be due to incorporation of hybrid composite which enhanced electrochemical properties of N-MWCNT surface[46–49].

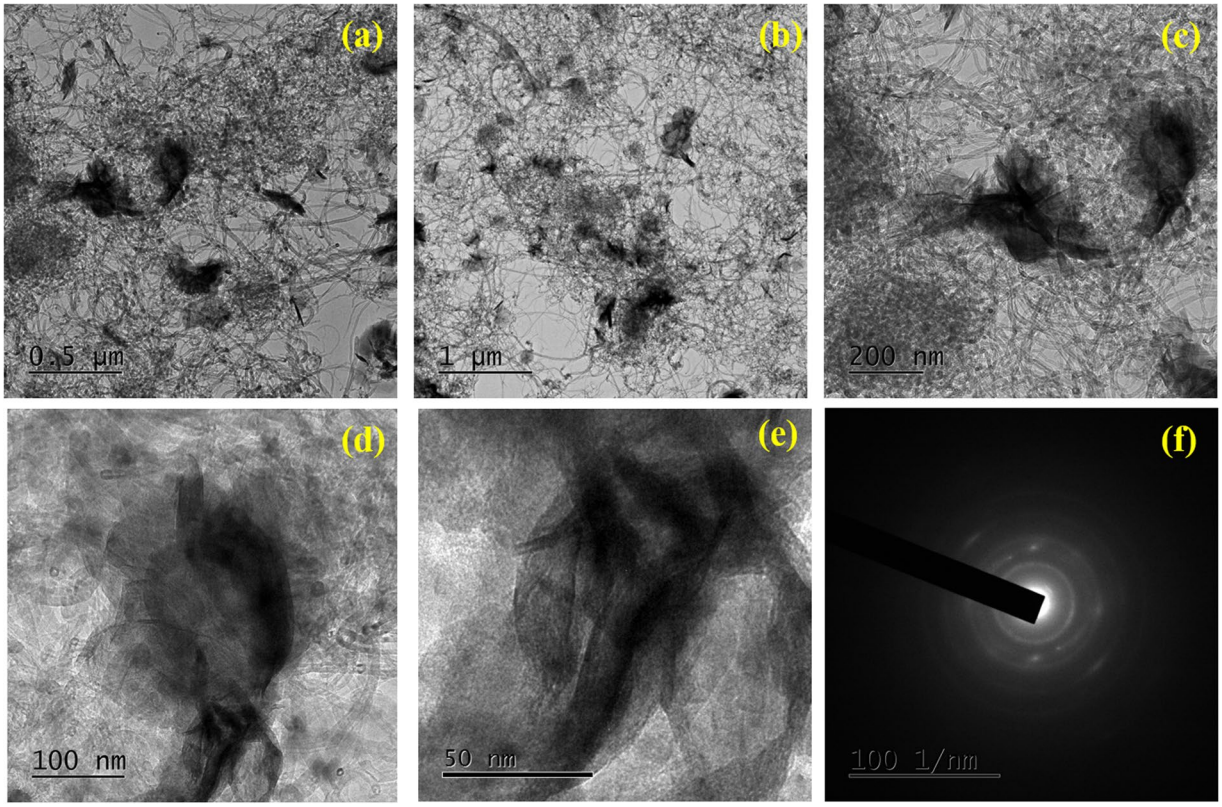

Figure 6. (**a**–**e**)HR-TEM images and (**f**) SAED pattern of the Ni $(OH)_2$ @ N-MWCNT.

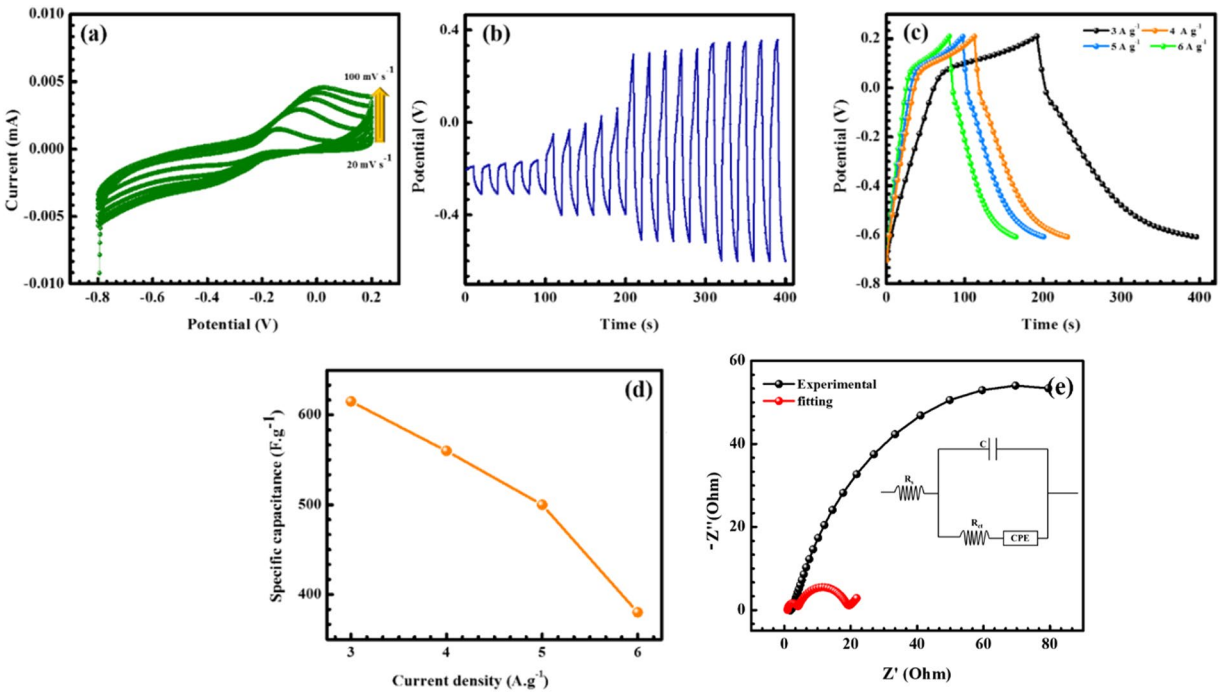

Figure 7. (**a**) CV at different scan rates (**b**) I vs t curve (**c**) GCD curve at different current densities (**d**) Capacitance at different current rates (**e**) EIS spectrum of $Ni(OH)_2$ @N-MWCNT.

Cyclic stability is an important factor for electrode performance of supercapacitor in the electrochemical reaction via three-electrode system. As shown in Fig. 7b, the stability of hybrid composite as an electrode material was studied by repeating continuous galvanic-charge discharge (GCD) of 3 A g^{-1} for 5000 cycles. The GCD cycles

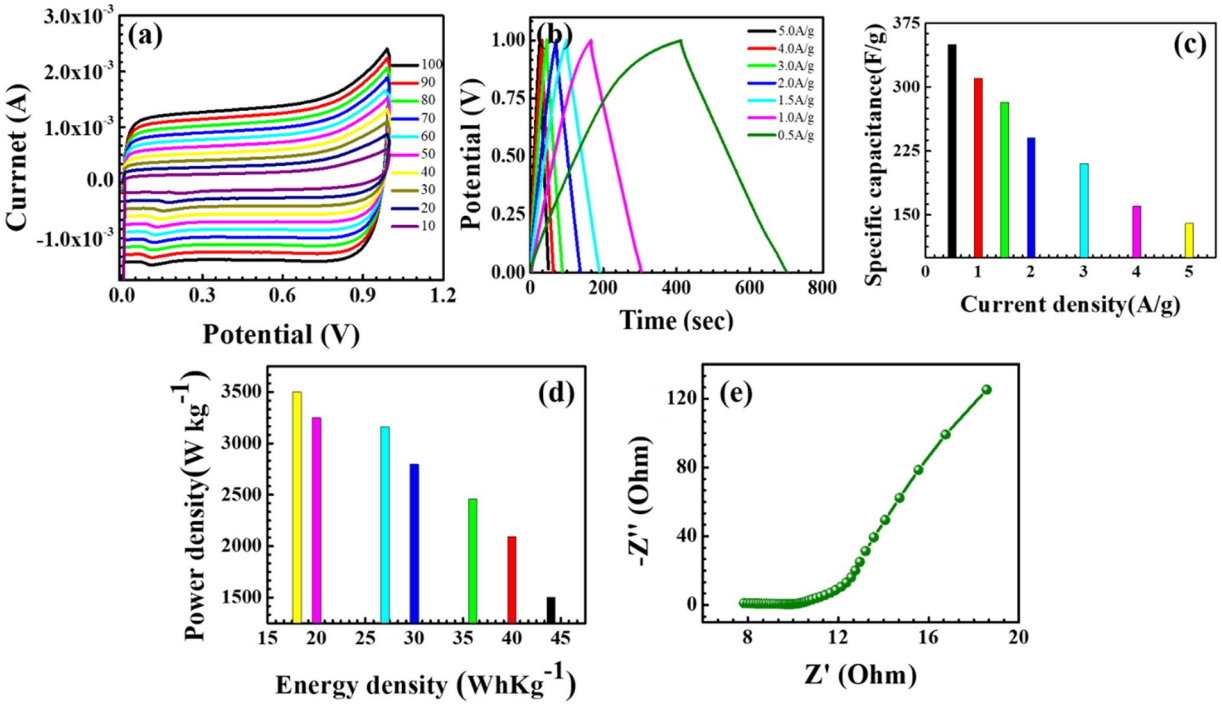

Figure 8. Asymmetric capacitor properties. (**a**) CV at different scan rates, (**b**) GCD curve at different current densities, (**c**) Capacitance at different current rates, (**d**) energy density vs. power density, (**e**) EIS spectrum of $Ni(OH)_2$ @N-MWCNT.

of the hybrid composite electrode retained about ~90% of its initial specific capacitance after 5000 cycles, demonstrating its excellent cyclic stability. The high capacitance retention implies that the hybrid composite electrode is a suitable material for high performance energy storage devices.

In addition, the flexible solid state asymmetric supercapacitor device used to study the $Ni(OH)_2$ @N-MWCNT hybrid composite electrode for practical applications. $Ni(OH)_2$ @N-MWCNT hybrid composite asymmetric results are shown in Fig. 8(a–e). The CV curves in the potential window between 0 and 1.2 V at different scan rates are displayed in the Fig. 8(a). When the scan rates increase from 10 to 100 mV s^{-1}, the shapes of CV curves are similar which indicating the good rate capability of the prepared electrodes. The electrochemical properties of the as-prepared ASC device was further evaluated by GCD tests at different current densities of 0.5 to 5 A/g, as shown in Fig. 8(b). The specific capacitance of the $Ni(OH)_2$ @N-MWCNT hybrid composite ASC device can be calculated based on the loading mass of the active materials (Fig. 8(c)). The specific capacitances are found to be ~350, 315, 282, 240, 210, 160 and 140 F g^{-1} at the current densities of 0.5,1, 1.5, 2, 3, 4 and 5 A g^{-1} respectively, and retains 90% of its initial capacitance after 5000 cycles at a current of 0.5 A g^{-1}. Figure 8(d) shows the Ragone plots that compares the power density and energy density[50,51]. It is quite observed from the Fig. 8(d) that the ASC shows the maximum energy density of ~43.75 Wh kg^{-1} with a power density of 1500 W kg^{-1} at 0.5 A g^{-1}. Its relative nyquist impedance plot is provided in Fig. 8(e). In this asymmetric electrode device even at high current density of 5 A g^{-1}, the energy density maintains at 17.50 Wh kg^{-1} at a power density of 3500 W kg^{-1} which suggests that the prepared composite electrodes could be utilized as a prime candidate in conventional electrochemical energy storage devices.

Conclusions

In summary, $Ni(OH)_2$@N-MWCNT hybrid composite was successfully synthesized *via* thermal reduction process. In this process, CTAB was an important surfactant to avoid agglomeration of nickel hydroxide particles. XRD diffraction peaks were proved to be hexagonal phase of β-Ni $(OH)_2$. There was no impurity in the hybrid composite. BET surface area of the hybrid composite was ~250 m^2 g^{-1}, greater than pristine $Ni(OH)_2$ sample (~108 m^2 g^{-1}). The hybrid composite showed wide pore size distribution with particle size of ~1.5–20 nm. The specific capacitance of the $Ni(OH)_2$ @N-MWCNT hybrid composite showed the maximum specific capacitance of ~350 F g^{-1} at 0.5 A g^{-1} and retains 90% of initial capacitance after 5000 cycles. This can facilitate the migration of ions in presence of 6 M KOH electrolyte during the charge/discharge process. After 5000 cycles, only 10% of its initial capacitance was lost, demonstrating its good cyclic stability which in turn favors the way to utilize as potential candidate in high performance supercapacitors.

Materials and Methods

All chemicals and reagents were used without any distillation process. Multiwalled carbon nanotubes (MWCNT-CMP-310F, Size 10–20 nm) were purchased from Lijiang Nanotech Co. Ltd, South Korea. Nickel nitrate $Ni(NO_3)_2{\cdot}6H_2O$, potassium permanganate ($KmnO_4$), urea (Sigma-Aldrich, 98%), cetyltriemthyl

ammonium bromide (CTAB), Sulfuric acid (H_2SO_4,), ammonium hydroxide (NH_4OH), potassium hydroxide (KOH), polytetrafluorethylene (PTFE), Poly vinyl alcohol (PVA)MW = 77,000 were collected from Aldrich chemical company, South Korea.

Synthesis of nitrogen doped N-MWCNT. Typical synthetic methods used to dope MWCNT materials with N include high-temperature arc-discharge process, CVD, solvothermal process (200–300 °C) and laser ablation methods were reported in detail[52–54]. Based on the thermal reduction chemical process of MWCNT synthesis as follows. MWCNT (3 g) was dispersed in DI water followed by well sonication for 2 h. The reaction solution was then added with 20 ml of ammonia and 1.2 g of urea followed by continuous stirring at 95 °C for 10 h. The resultant product of N-doped MWCNT was calcined at 350 °C for 8 h. Samples were then collected for further study.

Synthesis of Ni $(OH)_2$@N-MWCNT decorated hybrid composite. N-MWCNT (0.25 g) was taken in to 500 ml beaker and required 100 ml of distilled water then continuously stirred for 1 h at 95 °C. Stoichiometric amounts of $Ni(NO_3)_2{\cdot}6H_2O$ (0.74 g), cetyl ammonium bromide (1 g) and urea (0.9 g) were then added into the MWCNT solution and stirred at 95 °C. Initially, the solution became turbid due to formation of $Ni(OH)_2$ which was dissolved by addition of surfactant. Afterwards, the resulting transparent solution was kept under *vacuum* in a vacuum oven at 95 °C for 12 h. The resulting composite material was purified by ethanol followed by calcination at 450 °C for 8 h. Finally, hybrid composite samples were collected and stored in a desiccator to prevent moisture effect.

Materials characterization. $Ni(OH)_2$ @N-MWCNT hybrid composites were characterized by FTIR and RM200 confocal Raman spectro microscopy scanned in the range of 100 to 400 cm^{-1} in the presence of He and Ni laser beam source. XRD pattern of hybrid composite was studied using Rigaku Rotaflex (RU-200B) X-ray diffractometry in presence of Cu K_α radiation source. Morphology of the electrode was characterized by FE-TEM analysis using JEM-2010F (Hitachi S-4800, Japan). XPS analysis of hybrid composite was performed using XPS, ESCALAB 250Xi (Thermo Fisher Scientific, USA) in the presence of Al Kα radiation. Electrochemical properties of the hybrid composite were evaluated with CHI 760D (CH instrument Inc.). CV experiments were performed with the three-electrode system in the presence of 6 M KOH as strong electrolyte solution. In these experiments, the potential ranged from −0.8 to 0.2 SCE at a series of scan rates (20 to 100 mV/s). GCD curves occurred at various current densities (3, 4, 5 and 6 A/g) in the range of potential (−0.8 to 0.2). EIS analysis was characterized by using the experimental range of 0.1 Hz to 100 KHz and referring to open circuit potential. The electrochemical properties of the asymmetric cells were studied through cyclic voltammetry (CV), GCD, and EIS analyses via (VersaSTAT3 electrochemical workstation, Princeton, USA). The two-electrode system configured as counter electrode is connected together with reference electrode at same terminal.

Electrode preparation. A conventional three-electrode system (CHI 760D, CH instrument Inc.) was used to characterize $Ni(OH)_2$ @N-MWCNT hybrid composites in presence of 6 M KOH electrolyte solution. In this experiment, active material as a working, Pt wire utilize (counter) and reference electrodes (Ag/AgCl) for CV analysis. These working electrodes were fabricated by coating Ni wire electrode with 75 wt% active materials, 20 wt% conductive agent (carbon black) and 5 wt% polyvinylidene fluoride (PVDF) using N-methylpyrrolidone (NMP) as solvent. Electrochemical performance of the prepared hybrid composite was determined using cyclic voltammetry (CV) (20–100 mV/s), galvanostatic charge-discharge (GCD) (3 to 6 A g^{-1}) and electrochemical impedance spectroscopy (EIS) measurements (0.1 Hz to 100 KHz). Results are discussed in the following sections.

The asymmetric device were fabricated as following methods: $Ni(OH)_2$ @N-MWCNT hybrid composites electrodes were placed in the parallel and calculated 500 μm apart, then fixed with tape and inserted into a glass tube complete with 6 M KOH electrolyte. The KIMTECH paper was soaked in 6 M KOH solution and acted as the separator. The two electrodes were prepared by using a hybrid composite, conductive carbon black, and PTFE in the mass ratio of 85:10:5. The obtained slurry was then coated onto carbon fiber paper (with an active area of exactly 1 cm^2) and dried at 90 °C for 30 min. The mass of hybrid composite electrodes E_1 and E_2 was 14 mg and 10 mg, respectively.

References

1. Miller, J. R. *et al*. Graphene Double-Layer Capacitor with ac Line-Filtering Performance. *Science (80-.).* **329**, 1637–1639 (2010).
2. Wang, H., Casalongue, H. S., Liang, Y. & Dai, H. $Ni(OH)_2$ Nanoplates Grown on Graphene as Advanced Electrochemical Pseudocapacitor Materials. *J. Am. Chem. Soc.* **132**, 7472–7477 (2010).
3. Wang, G., Zhang, L. & Zhang, J. A review of electrode materials for electrochemical supercapacitors. *Chem. Soc. Rev.* **41**, 797–828 (2012).
4. Emmenegger, C. *et al*. Investigation of electrochemical double-layer (ECDL) capacitors electrodes based on carbon nanotubes and activated carbon materials. *J. Power Sources* **124**, 321–329 (2003).
5. Ferrero, G. A., Fuertes, A. B. & Sevilla, M. N-doped microporous carbon microspheres for high volumetric performance supercapacitors. *Electrochim. Acta* **168**, 320–329 (2015).
6. Le, Q., Wang, T., Zhu, S., Zhang, J. & Zhang, Y. Facile synthesis of carbon sphere@Ni(OH) $_2$ and derivatives for high-performance supercapacitors. *Funct. Mater. Lett.* **09**, 1642002 (2016).
7. Arul, N. S. & Han, J. I. Enhanced pseudocapacitance of NiSe2/Ni(OH)2 nanocomposites for supercapacitor electrode. *Mater. Lett.* **234**, 87–91 (2019).
8. Zhang, Y. X. *et al*. Hierarchical NiO moss decorated diatomites via facile and templated method for high performance supercapacitors. *Mater. Lett.* **120**, 263–266 (2014).
9. Kirubasankar, B., Palanisamy, P., Arunachalam, S., Murugadoss, V. & Angaiah, S. 2D MoSe2-Ni(OH)2 nanohybrid as an efficient electrode material with high rate capability for asymmetric supercapacitor applications. *Chem. Eng. J.* **355**, 881–890 (2019).
10. Xu, Y. *et al*. Holey graphene frameworks for highly efficient capacitive energy storage. *Nat. Commun.* **5**, 4554 (2014).

11. Zhi, M., Xiang, C., Li, J., Li, M. & Wu, N. Nanostructured carbon–metal oxide composite electrodes for supercapacitors: a review. *Nanoscale* **5**, 72–88 (2013).
12. Vijayakumar, S., Nagamuthu, S. & Muralidharan, G. Supercapacitor Studies on NiO Nanoflakes Synthesized Through a Microwave Route. *ACS Appl. Mater. Interfaces* **5**, 2188–2196 (2013).
13. Saravanakumar, B., Purushothaman, K. K. & Muralidharan, G. Interconnected V_2O_5 Nanoporous Network for High-Performance Supercapacitors. *ACS Appl. Mater. Interfaces* **4**, 4484–4490 (2012).
14. Wu, G. *et al*. High-performance Supercapacitors Based on Electrochemical-induced Vertical-aligned Carbon Nanotubes and Polyaniline Nanocomposite Electrodes. *Sci. Rep.* **7**, 43676 (2017).
15. Cao, P., Wang, L., Xu, Y., Fu, Y. & Ma, X. Facile hydrothermal synthesis of mesoporous nickel oxide/reduced graphene oxide composites for high performance electrochemical supercapacitor. *Electrochim. Acta* **157**, 359–368 (2015).
16. Liao, Q., Li, N., Jin, S., Yang, G. & Wang, C. All-Solid-State Symmetric Supercapacitor Based on Co_3O_4 Nanoparticles on Vertically Aligned Graphene. *ACS Nano* **9**, 5310–5317 (2015).
17. Ding, S. *et al*. Controlled synthesis of hierarchical NiO nanosheet hollow spheres with enhanced supercapacitive performance. *J. Mater. Chem.* **21**, 6602 (2011).
18. Sun, X., Wang, G., Hwang, J.-Y. & Lian, J. Porous nickel oxide nano-sheets for high performance pseudocapacitance materials. *J. Mater. Chem.* **21**, 16581 (2011).
19. Ramesh, S., Haldorai, Y., Sivasamy, A. & Kim, H. S. Nanostructured Co3O4/nitrogen doped carbon nanotube composites for high-performance supercapacitors. *Mater. Lett.* **206**, 39–43 (2017).
20. Jiang, Y. *et al*. A facile hydrothermal synthesis of graphene porous NiO nanocomposite and its application in electrochemical capacitors. *Electrochim. Acta* **91**, 173–178 (2013).
21. Ke, Q. *et al*. Surface-Charge-Mediated Formation of H-TiO_2@$Ni(OH)_2$ Heterostructures for High-Performance Supercapacitors. *Adv. Mater.* **29**, 1604164 (2017).
22. Vijayakumar, S. & Muralidharan, G. Electrochemical supercapacitor behaviour of α-Ni(OH)2 nanoparticles synthesized via green chemistry route. *J. Electroanal. Chem.* **727**, 53–58 (2014).
23. Huang, Q. *et al*. Nickel hydroxide/activated carbon composite electrodes for electrochemical capacitors. *J. Power Sources* **164**, 425–429 (2007).
24. Wang, D.-W., Li, F. & Cheng, H.-M. Hierarchical porous nickel oxide and carbon as electrode materials for asymmetric supercapacitor. *J. Power Sources* **185**, 1563–1568 (2008).
25. Zhang, H. *et al*. One-Step Electrophoretic Deposition of Reduced Graphene Oxide and $Ni(OH)_2$ Composite Films for Controlled Syntheses Supercapacitor Electrodes. *J. Phys. Chem. B* **117**, 1616–1627 (2013).
26. Ji, J. *et al*. Nanoporous $Ni(OH)_2$ Thin Film on 3D Ultrathin-Graphite Foam for Asymmetric Supercapacitor. *ACS Nano* **7**, 6237–6243 (2013).
27. Li, F. *et al*. Reduction of Graphene Oxide with Ni Powder for the Preparation of Ni(OH)₂/Reduced Graphene Oxide Hybrid Electrodes for Supercapacitors. *Sci. Adv. Mater.* **7**, 269–277 (2015).
28. Ramesh, S., Vikraman, D., Kim, H.-S., Kim, H. S. & Kim, J.-H. Electrochemical performance of MWCNT/GO/NiCo2O4 decorated hybrid nanocomposite for supercapacitor electrode materials. *J. Alloys Compd.* **765**, 369–379 (2018).
29. Yun, J., Kim, D., Lee, G. & Ha, J. S. All-solid-state flexible micro-supercapacitor arrays with patterned graphene/MWNT electrodes. *Carbon N. Y.* **79**, 156–164 (2014).
30. Yang, Z. *et al*. Recent Advancement of Nanostructured Carbon for Energy Applications. *Chem. Rev.* **115**, 5159–5223 (2015).
31. Wang, Y. *et al*. High-Performance Flexible Solid-State Carbon Cloth Supercapacitors Based on Highly Processible N-Graphene Doped Polyacrylic Acid/Polyaniline Composites. *Sci. Rep.* **6**, 12883 (2016).
32. Lee, J. W., Ko, J. M. & Kim, J.-D. Hierarchical Microspheres Based on α-$Ni(OH)_2$ Nanosheets Intercalated with Different Anions: Synthesis, Anion Exchange, and Effect of Intercalated Anions on Electrochemical Capacitance. *J. Phys. Chem. C* **115**, 19445–19454 (2011).
33. Hyder, M. N. *et al*. Layer-by-Layer Assembled Polyaniline Nanofiber/Multiwall Carbon Nanotube Thin Film Electrodes for High-Power and High-Energy Storage Applications. *ACS Nano* **5**, 8552–8561 (2011).
34. Zhu, G. *et al*. Polymer guided synthesis of Ni(OH)2 with hierarchical structure and their application as the precursor for sensing materials. *CrystEngComm* **15**, 9189 (2013).
35. Trung, N. B. *et al*. Facile synthesis of three-dimensional graphene/nickel oxide nanoparticles composites for high performance supercapacitor electrodes. *Chem. Eng. J.* **264**, 603–609 (2015).
36. Ganesh, V., Pitchumani, S. & Lakshminarayanan, V. New symmetric and asymmetric supercapacitors based on high surface area porous nickel and activated carbon. *J. Power Sources* **158**, 1523–1532 (2006).
37. Wu, M.-S. & Hsieh, H.-H. Nickel oxide/hydroxide nanoplatelets synthesized by chemical precipitation for electrochemical capacitors. *Electrochim. Acta* **53**, 3427–3435 (2008).
38. Lee, J. Y., Liang, K., An, K. H. & Lee, Y. H. Nickel oxide/carbon nanotubes nanocomposite for electrochemical capacitance. *Synth. Met.* **150**, 153–157 (2005).
39. Cheng, J., Cao, G.-P. & Yang, Y.-S. Characterization of sol–gel-derived NiOx xerogels as supercapacitors. *J. Power Sources* **159**, 734–741 (2006).
40. Chen, H., Zhou, M., Wang, Z., Zhao, S. & Guan, S. Rich nitrogen-doped ordered mesoporous phenolic resin-based carbon for supercapacitors. *Electrochim. Acta* **148**, 187–194 (2014).
41. Zheng, Y., Ding, H. & Zhang, M. Preparation and electrochemical properties of nickel oxide as a supercapacitor electrode material. *Mater. Res. Bull.* **44**, 403–407 (2009).
42. Liang, K., Tang, X. & Hu, W. High-performance three-dimensional nanoporous NiO film as a supercapacitor electrode. *J. Mater. Chem.* **22**, 11062 (2012).
43. Fan, L., Tang, L., Gong, H., Yao, Z. & Guo, R. Carbon-nanoparticles encapsulated in hollow nickel oxides for supercapacitor application. *J. Mater. Chem.* **22**, 16376 (2012).
44. He, X. *et al*. Hierarchical FeCo2O4@NiCo layered double hydroxide core/shell nanowires for high performance flexible all-solid-state asymmetric supercapacitors. *Chem. Eng. J.* **334**, 1573–1583 (2018).
45. Bittencourt, C. *et al*. Decorating carbon nanotubes with nickel nanoparticles. *Chem. Phys. Lett.* **436**, 368–372 (2007).
46. He, X. *et al*. High-performance all-solid-state asymmetrical supercapacitors based on petal-like NiCo2S4/Polyaniline nanosheets. *Chem. Eng. J.* **325**, 134–143 (2017).
47. Xing, W., Li, F., Yan, Z. & Lu, G. Q. Synthesis and electrochemical properties of mesoporous nickel oxide. *J. Power Sources* **134**, 324–330 (2004).
48. Duraisamy, N. *et al*. Investigation on structural and electrochemical properties of binder free nanostructured nickel oxide thin film. *Mater. Lett.* **161**, 694–697 (2015).
49. Ge, D. *et al*. Foldable supercapacitors from triple networks of macroporous cellulose fibers, single-walled carbon nanotubes and polyaniline nanoribbons. *Nano Energy* **11**, 568–578 (2015).
50. Zhao, Y. *et al*. Hierarchical NiCo2S4@CoMoO4 core-shell heterostructures nanowire arrays as advanced electrodes for flexible all-solid-state asymmetric supercapacitors. *Appl. Surf. Sci.* **453**, 73–82 (2018).
51. Zhao, Y. *et al*. A flexible all-solid-state asymmetric supercapacitors based on hierarchical carbon cloth@CoMoO4@NiCo layered double hydroxide core-shell heterostructures. *Chem. Eng. J.* **352**, 29–38 (2018).

52. Ramesh, S., Kathalingam, A., Karuppasamy, K., Kim, H.-S. & Kim, H. S. Nanostructured CuO/Co2O4@ nitrogen doped MWCNT hybrid composite electrode for high-performance supercapacitors. *Compos. Part B Eng.* **166**, 74–85 (2019).
53. Mo, Z., Liao, S., Zheng, Y. & Fu, Z. Preparation of nitrogen-doped carbon nanotube arrays and their catalysis towards cathodic oxygen reduction in acidic and alkaline media. *Carbon N. Y.* **50**, 2620–2627 (2012).
54. Szabó, A. *et al*. Synthesis Methods of Carbon Nanotubes and Related Materials. *Materials (Basel).* **3**, 3092–3140 (2010).

Acknowledgements

This research was fully supported by Basic Science Research Program through National Research Foundation (NRF-2017R1D1A1B03028368), under the Ministry of Education, and Institute for Information & communications Technology Promotion (IITP) grant funded by the Korea government (MSIP) (No. R75201600050001002) and also supported under the framework of 2017 international cooperation program (GRDC- INHA IST-NASA Joint Research Center) through National Research Foundation by Ministry of Science and ICT of Korea (Grant No: 2017K1A4A3013662).

Author Contributions

S.R., K.K. and H.S.K. design the project and the experiments. S.R. and K.K. carried out the experiments. All authors S.R., K.K., H.M.Y., J.-J.L., H.-S.K., H.S.K. and J.-H.K. involved to the characterization of the materials and the discussions prominent up to the writing of the manuscript. S.R. and H.S.K. took part in the main discussions that led to the final manuscript; all authors read and finalized the final manuscript.

Additional Information

Competing Interests: The authors declare no competing interests.

Publisher's note: Springer Nature remains neutral with regard to jurisdictional claims in published maps and institutional affiliations.